LARGE-EDDY SIMULATION OF NOISE RADIATED BY A MACH 0.9 ROUND JET AT HIGH REYNOLDS NUMBER

Carlos A. S. Moser, carlos.moser@yahoo.com.br
Marcello A. F. Medeiros, marcello@sc.usp.br
Dept. Aeronautical Engineering, EESC/USP, São Carlos SP - Brazil

Jorge H. Silvestrini, jorgehs@pucrs.br
Dept. Mechanical and Mechatronics Engineering, PUCRS, Porto Alegre RS - Brazil

Abstract. *The aerodynamic noise radiated by a subsonic round jet at high Reynols number was investigated by an implicit large-eddy simulation (LES) method based on the approximate deconvolution model (ADM). Unlike the traditional eddy-viscosity type models, the LES/ADM approach assumes that the subgrid-scale model may be determined by the resolved scales of the flow and, therefore, does not require any additional subgrid-scale stress and heat flux terms in the flow equations. This approach also preserves the Reynolds number of the jet, which might not be possible using eddy-viscosity models. The flow variables were solved in Cartesian coordinates by the non-conservative form of the fully compressible Navier-Stokes equations. The major advantage of using a non-conservative formulation is that it avoids the inconsistent treatment of density weighting (or Favre avareging) of flow variables, commonly used in LES of unsteady flows with rapid property variations, such as compressible free-shear layer flows. The large difference of scales between the flow and the acoustic field was solved using high-order accurate compact finite difference schemes for spatial discretization and implicit filtering, and a fourth-order Runge-Kutta method for time integration. Non-reflecting boundary conditions and buffer zone treatments were prescribed by a characteristic-based formulation and a conceptual model based on the characteristic analysis. Implicit LES of the well-known test case of a Mach* 0.9 *round jet at Reynolds number* 6.5×10^4 *were carried out by a high performance multi-block message passing interface (MPI) parallel solver with finite-sized overlap inter-block communication. An extensive investigation of the round jet was perfomed, in particular for the analysis of jet flow dynamic characteristics, such as the shear-layer thickness, mean velocity decaying and jet spreading. The flow-noise sources and the acoustic field propagation where directly computed by implicit LES without any modeling assumption. Preliminary results were found to be in good agreement with previous numerical results and experimental data at similar flow conditions. In the ongoing work, it is hoped that well-resolved MPI parallel computations of jet flow-noise sources and its inherently coupled noise radiation will allow us to investigate more deeply the underlying nonlinear mechanisms by which noise is aerodynamically generated by free shear-layer flows.*

Keywords: *Computational Aeroaacoustics, Aerodynamic Noise Radiation, Implicit Large-Eddy Simulation, Approximate Deconvolution Model, Message Passing Interface*

1. INTRODUCTION

The noise radiated from an extensive region of unsteady hydrodynamics was firstly investigated by Colonius, T. and Lele, S. K. and Moin P. (1997) by performing direct numerical simulation (DNS) of a two-dimensional (2D) mixing layer. They found that the presence of flow-acoustic interactions was very sensitive to small changes in the computed flow-noise source. By performing DNS to compute the sound radiated from subsonic and supersonic axisymmetric 2D jets, Mitchell, B. E. and Lele, S. K. and Moin P. (1999) found good agreement with predictions of Lighthill's acoustic analogy (Lighthill, 1952). However, because of the inherently high computational cost, DNS is restricted to flows in the low Reynolds number regime. At high Reynolds numbers, large-eddy simulation (LES) can be employed as a less expensive alternative approach, since only the filtered large scales are fully resolved, while the effects of the smallest unresolved subgrid scales are modeled or reconstructed.

In the last few years, LES has achieved significant progress due to advances in computational power, numerical algorithms and subgrid-scale models. LES has been applied to a wide variety of turbulent flows, ranging from problems of scientific interest to those with engineering applications. This trend has been motivated by the need to provide a more realistic characterization of complex unsteady flows encountered in areas such as flow control, aeroacoustics and fluid/structure interaction. However, the vast majority of LES research has been devoted to incompressible flows; while compressible flow applications have only recently gained some attention, due to the increased complexity introduced by the need to model the energy equation. Ideally, for incompressible flows the filtering of the Navier-Stokes equations generates a closure problem in the form of an unknown residual subgrid-scale stress tensor:

$$\tau_{i,j} = \overline{u_i u}_j - \bar{u}_i \bar{u}_j. \tag{1}$$

The filtering equations are not closed because of the nonlinear term $\overline{u_i u}_j$, since the subgrid-scale tensor stems from a closure problem introduced by the spatial filtering operation and not from the discretization's inability to represent the

small scales in the flow. As a result, the stress tensor strongly depends on the assumed filter shape, which causes a subgrid-scale model to be inherently filter dependent. Hence, depending on the choice of the filter, the corresponding model should satisfy very different requirements in terms of large-scale dynamics and kinetic energy budget.

LES methods for compressible flows have ranged from the inherently limited Smagorinsky eddy-viscosity type models to more sophisticated and accurate dynamic models. The Smagorinsky-type models exhibit two major drawbacks. They ignore turbulence anisotropy and use a local balance assumption between the subgrid-scale turbulence kinetic energy production and its dissipation. Furthermore, they predict non-vanishing subgrid eddy viscosity in regions where the flow is laminar. Moreover, since eddy viscosity has the same functional form as molecular viscosity, it is difficult to preserve the effective Reynolds number of the simulated flow. The dynamic procedures (Germano, M. and Piomelli, U. and Moin, P., 1991; Lilly, D., 1992) for computing the model coefficient, which does not require adjustable constant, overcome these shortcomings. Nevertheless, the numerical stabilization become complicated when the dynamic model is applied to flows in which there are inhomogeneous directions. Vreman, A. W. (2004a) developed a subgrid eddy-viscosity type model especially suitable for laminar shear flows, since it vanishes subgrid dissipation in laminar regions and does not require any averaging or clipping procedure for numerical stabilization. Park, N. and Lee, S. and Choi, H. (2006) proposed a dynamic procedure for determining the model coefficient utilizing the global equilibrium between the subgrid and viscous dissipation. In this approach, the model coefficient is globally constant in space but varies in time, and still garantees zero eddy viscosity in the laminar flow regions. Bogey, C. and Bailly, C. (2003a) employed a LES approach based on the Smagorinsky model to compute the aerodynamic noise radiated by a Mach 0.9 jet at Reynolds number 6.5×10^4. The mean flow and turbulence intensities, as well as sound directivity and sound levels, were found to be in good agreement with experimental data. Bodony, D. J. and Lele, S. K. (2005) conducted a systematic investigation of LES's capability for jet noise predictions at the Reynolds number range from 1.3×10^4 to 3.36×10^5. Noise predictions for the unheated and heated jets were found to be in agreement with experimental data (Tanna, H. K., 1977). Bogey, C. and Bailly, C. (2006) observed that the spatial structure of inflow disturbances can significantly impact the jet flow development and the radiated noise predicted by compressible LES at high Reynolds numbers. The pronounced sensitivity of jets to variations of the inflow conditions has been demonstrated experimentally (Brown, 2005; Zaman, K.B.M.Q., 1985) as well as numerically (Stanley and Sarkar, 2000; Bogey, C. and Bailly, C., 2005). Some attempts on round jets at higher Reynolds number have been made by Choi, D. and Barber, T. J. and Chiappetta, L. M. (1999) and Boersma, B. J. and Lele, S. K. (1999). Nevertheless, except for some studies (Bogey, C. and Bailly, C., 2002, 2003b; Bogey, C. and Bailly, C. and Juvé, D., 2003; Bodony, D. J. and Lele, S. K., 2005) the highest Reynolds numbers reached by LES are still far bellow those of practical interest.

2. IMPLICIT LES METHODOLOGY

As an alternative approach to the traditional LES methods based on eddy-viscosity type models, in this work was developed an implicit LES methodology based on the approximate deconvolution model (ADM) (Stolz, S. and Adams, N.A., 1999) to compute the noise radiated by subsonic jets at high Reynolds number. High-order spatial filters (Gaitonde, D. V. and Visbal, M. R., 1999) were used to implicitly model the energy content present in the poorly resolved smallest scales of the flow. This aproach does not require any additional subgrid scale stress or heat flux terms in the flow equations. Although the filter is applied explicitly to the evolving solution, this approach is referred as implicit LES, since the application of the spatial filter is a fundamental component to mantain stability by removing high-frequency spurious numerical oscillations. The basis of this approach is that the numerical truncation error associated with the discretization has similar form or action to the subgrid scale model. Such approach falls into the class of structural models, since there is no assumed form of the subgrid flow and the subgrid model is entirely determined by the structure of the resolved flow (Sagaut, P., 2001). Nevertheless, even with the recently increase of interest in implicit LES, there is not a consensus on the appropriate form of the discretization error, since it is assumed that the numerics provide sufficient modeling of the subgrid terms to allow correct dissipation of turbulent kinetic energy.

In order to satisfy stringent requirements of aeroacoustic computations, such as the large difference of scales between the flow and the acoustic field, high-order compact finite difference schemes were used for spatial discretization and implicit filtering, and a fourth-order Runge-Kutta method for time integration. In principle, to mantain acceptable numerical acurracy and proper resolution of low wavenumbers, the filter accuracy should be equal or greater than the corresponding accuracy of the spatial discretization scheme. Thus, the flow variables were sequentially filtered in every spatial direction at the final stage of each time step with sixth-order implicit filters (Gaitonde, D. V. and Visbal, M. R., 1999). The analysis of the impact of spatial discretization errors on the filtered solution establishes the need of high-order spatial filtering. The high-order filtering of the compressible Navier-Stokes equations should provides dissipation at the higher modified wave numbers only, where the spatial discretization already exhibits significant dispersion errors, and enforce numerical stability on nonuniform grids. The filtering also should eliminate numerical instabilities arising from poor grid quality, unresolved scales, or boundary conditions, which left to grow can potentially corrupt the flow solution.

2.1 High-Order Implicit Filtering

The filtering operation is defined by Leonard, A. (1974) in the physical space as

$$\bar{f}(x) = \int_{\Omega} f(x')G(x, x'; \delta)dx' \tag{2}$$

where Ω is the entire domain, G is the filter kernel and δ is the filter width associated to the smallest scales retained by the filtering operation. Thus, $\bar{f}$ defines the size and structure of the small scales.

The flow solution was computed by the non-conservative form of the fully compressible Navier-stokes equations, which does not require the density-weighting or Favre filtering average. Sixth-order compact finite difference schemes (Lele, S. K., 1992) were employed for spatial discretization and a fourth-order Runge-Kutta method was used for time integration.

At the interior grid points $i = 4, ..., N-3$, the implicit filtering approach is defined as follows

$$\alpha_f \bar{f}_{i-1} + \bar{f}_i + \alpha_f \bar{f}_{i+1} = \sum_{n=1}^{4} \frac{a_n}{2}(f_{i-n+1} + f_{i+n-1}) \tag{3}$$

where the coefficients a_n are derived in terms of the filtering parameter α_f by Taylor and Fourier series analysis (Gaitonde, D. V. and Visbal, M. R., 1998, 1999), which must satisfy the inequality $-0.5 \leq \alpha_f \leq 0.5$. Filters less dissipative are obtained with higher values of α_f within the given range, and for $\alpha_f = 0.5$ there is no filtering effect. By contrast, for $\alpha_f = 0$ the explicit filtering operation displays significant degradation of the spectral frequency response. Here, α_f was fixed as 0.40. However, filters less dissipatives with larger values of α_f will be tested in future works.

As equation (3) has a right-hand side stencil of seven points, obviously it can not be employed near the boundaries of the domain. Thus, the following implicit filter was used at the grid points $i = 2$ and 3:

$$\alpha_f \bar{f}_{i-1} + \bar{f}_i + \alpha_f \bar{f}_{i+1} = \sum_{n=1}^{7} a_{n,i} f_n \tag{4}$$

and analogously, at the grid points $i = N-2$ and $N-1$. While at the boundary points $i = 1$ and N, the flow variables were kept without application of any filtering operation.

2.2 Approximate Deconvolution Model

An implicit LES approach re-interpreted in the context of an approximate deconvolution model (Stolz, S. and Adams, N.A., 1999) was used to compute the filtered solution variable $\bar{f}$ by the following filtering operation

$$\bar{f} = G * f = \int G(x - x')f(x')dx' \tag{5}$$

where G is the filter transfer function. By supposing that G has an inverse Q, an approximation of the unfiltered variable f, denoted by f^*, may be obtained by the deconvolution of the filtered variable $\bar{f}$ as

$$f^* = Q * \bar{f} \tag{6}$$

where the inverse filter transfer function Q may be obtained by the truncated power series expansion

$$Q_N = \sum_{\nu=0}^{N} (I - G)^{\nu} \tag{7}$$

where I is the identity matrix and $N = 1, 2, 3, ...$ the number of filtering steps. The family of inverse filter transfer functions, Q_N, is based on an iterative deconvolution method (Galdi, G. P., 2000). High-order approximations f^* from the unfiltered variable f, can be derived by sucessive filtering operations applied to the filtered quantities

$$f^* = \bar{f} + (I - G) * \overline{f} + (I - G) * ((I - G) * \overline{f}) + ... \tag{8}$$

In smooth regions of the flow, these filters have strong stability properties and high-order consistency error $O(\delta^{2N+2})$, where δ is the filter width. As reported by Stolz, S. and Adams, N.A. and Kleiser, L. (2001a), the truncation order of the Eq.(8) determines the level of deconvolution. Here we choose the third level quadratic extrapolation:

$$f^* \approx Q_2\overline{f} := 3\overline{f} - 3\overline{\overline{f}} + \overline{\overline{\overline{f}}} \tag{9}$$

since it affords a sufficiently high-order consistency error $O(\delta^5)$.

3. MULTI-BLOCK MPI PARALLEL SOLVER

As stated above, the main goal of the present work is to perform the implicit LES of the aerodynamic noise radiated by round jets at high Reynolds number. However, this task is difficult or almost impossible to be executed using a single-block domain sequential code, due to the large memory requirement and high computational cost of 3D aeroacoustic computations. Thus, a multi-block MPI parallel solver with finite-sized overlap interface communication was demeed to properly recover the interior high-order accuracy of the differencing and filtering schemes of the original single-block sequential solver. The accurate treatment of the interfaces between blocks is a major issue in multi-block domain computations. Interfaces with high overlap interface treatments have shown to be stable and accurate even for general curvilinear meshes and viscous flows, however they substantially increase the CPU time due to the increase of overlap interface communication. Therefore, in this work we chose to implement a multi-block MPI parallel processing strategy with one processor per block and nine-points overlap interface for inter-block communication.

To illustrate the data exchange between two adjacent blocks, in Fig. 1 are shown details of the single-block domain and the multi-block domain decomposition with nine-points overlap communication. The single-block domain is decomposed in two adjacent blocks L-1 and L, with nine-points overlap (depicted in blue). Data are exchanged between the two adjacent blocks at the end of every subtime-step, as well as after each application of the implicit filtering operation. In block L, the flow solution values at points 1 to 4 are set to be equal to the updated values at points N-8 to N-5 of block L-1. Similarly, the values of points N-3 to N of block L-1 are given through the points 6 to 9 of block L. The arrows indicate the data transfer direction at each point in the interface, except for the points in the middle of the overlap (points 5 and N-4), which are solved independently and do not transfer data directly from/to adjacent blocks. This dual solution facilitates detecting any "drift" between the solutions in the adjacent blocks, since at every subtime-step of the Runge-Kutta time integration method, the flow solution is advanced independently in each block in the same manner as in a single-block domain computation. In order to reduce memory allocatain on the multi-block parallel processing, each worker process is successively initialized by the master process with its corresponding portion of the single-block domain. Thus, the multi-block parallel solver needs only to allocate memory to the block which is being currently initialized by the master process. As the memory required by each worker process is inversely proportional to the number of blocks, this procedure substantially reduces the need of memory allocation, especially in 3D computations.

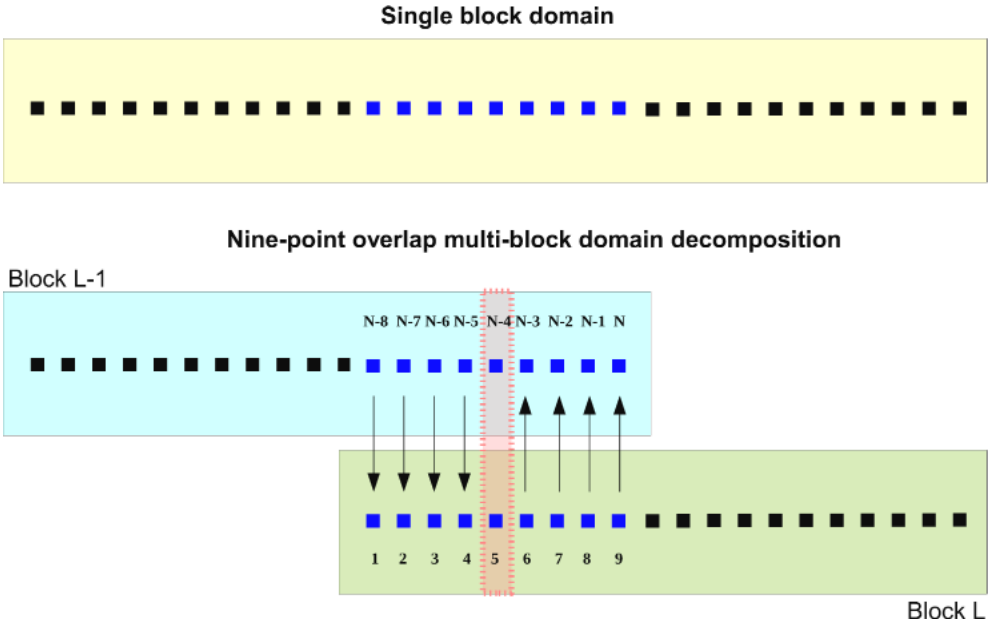

Figure 1. Schematic of a single block domain for sequential computation and a multi-block domain decomposition for MPI parallel processing with nine-points overlap interface communication. The arrows indicate the direction of data transfer between the adjacent blocks L-1 and L.

4. Jet flow configuration

In the implicit large-eddy simulation of the subsonic round jet, the jet nozzle exit has been modeled by imposing the following hyperbolic-tangent mean streamwise velocity profile

$$u_x(r) = \frac{U_j}{2}\left(1 + \tanh\left(\frac{r_o - r}{2\delta_\theta}\right)\right) \tag{10}$$

where U_j is the jet inlet centerline velocity, r_o is the jet radius and δ_θ is the shear-layer momentum thickness. For the present computations, the jet inlet transverse and spanwise velocities were set to zero. The Reynolds number $Re_D = U_j D/\nu$ was set to 6.5×10^4 and the Mach number to $M = U_j/c_o = 0.90$, where $D = 2r_o$ is the jet diameter, ν the kinematic viscosity and c_o the sound speed in the ambient medium. The choice of this Mach number may be justified by the considerable amount of numerical and experimental studies at similar flow conditions. The Reynolds number adopted is an intermediate value between jets obtained by DNS ($Re_D < 10^3$) and experimentally ($Re_D > 10^5$). The inlet momentum thickness was chosen as $\delta_\theta = 0.05 r_o$, to afford the development of turbulence after the jet nozzle exit and before the end of potential core. The mesh was discretized in Cartesian coordinates with $255^3 \approx 16.6$ million grid points. The physical domain extends to $50r_o$ in the streamwise direction and from $-25r_o$ to $25r_o$ in the transverse directions. To increase the dissipation of large-scales vortex structures of the flow before they interact with the outflow boundary, a buffer zone with grid stretching was attached just downstream of the physical domain until to $80r_o$.

4.1 Near-inflow forcing disturbance

In order to startup earlier the transition and seed turbulence in the jet shear layer, a low-amplitude random forcing disturbance of incompressible nature, i.e. with zero divergence (Bogey, C. and Bailly, C., 2005) was superimposed to the velocity field, just downstream of the jet inlet. This disturbance presents an axisymmetric structure of a vortex ring with velocity components

$$\left\{\begin{array}{c} u_{x_o} \\ u_{y_o} \\ u_{z_o} \end{array}\right\} = \frac{2r_o}{r\Delta_o}\ \exp\left[-\ln(2)\ \frac{\Delta_{x,r}^2}{\Delta_o^2}\right] \left\{\begin{array}{l} (r - r_o) \\ (x - x_o)\ \cos\ \gamma \\ (x - x_o)\ \sin\ \gamma \end{array}\right\} \tag{11}$$

where $\Delta_{x,r}^2 = (x - x_o)^2 + (r - r_o)^2$, $\gamma = \sin^{-1}(y/r)$ and $r = \sqrt{y^2 + z^2} \neq 0$. Δ_o is the minimum grid spacing in the jet shear layer and x_o the axial location of disturbance, chosen as $x_o = 0.80 r_o$.
The velocity fluctuations given by Eq.(11) were then superimposed onto the local flow velocity components

$$\left\{\begin{array}{c} u_x \\ u_y \\ u_z \end{array}\right\} = \left\{\begin{array}{c} u_x \\ u_y \\ u_z \end{array}\right\} + \left\{\begin{array}{c} u_{x_o} \\ u_{y_o} \\ u_{z_o} \end{array}\right\} U_j \sum_{i=0}^{n} \alpha_n \epsilon_n \cos(\theta_n + \phi_n) \tag{12}$$

where α_n, ϕ_n and θ_n are, respectively, the amplitude, phase and azimuthal angle of each one of the $n + 1$ modes of the disturbance. The parameters of the random disturbance were set as $\theta_n = n\theta$, $\epsilon_n = [-1, 1]$, $\phi_n = [0, \pi]$ and $\alpha_n = 2.5 \times 10^{-4}$, where n was set to 9.

4.2 Boundary conditions and buffer zone treatments

In present computations, the domain considered is large enough to allow wave propagation in the far-field, such that the deviations from the flow velocity fluctuations are likely to be small owing solely to acoustic fluctuations. Therefore, far-field non-reflecting boundary conditions were obtained by simply setting to zero the incoming waves at the outflow and lateral boundaries. Reflections of spurious waves generated by the disturbance at the inflow boundary were minimized by the application of a near-inflow absorbing zone (Moser, C. and Lamballais, E. and Gervais, Y., 2006).

Similarly to Colonius, T. and Lele, S. K. and Moin P. (1993), a buffer zone of aerodynamic dissipation was attached downstream of the physical domain to damp large-scale vortical structures originated by the turbulent flow. These structures are effectively dissipated in the buffer zone, before they interact with the outflow boundary, by adding artificial damping terms to the flow governing equations

$$\left.\frac{\partial \mathbf{Q}}{\partial t}\right|_{dp} = \frac{\partial \mathbf{Q}}{\partial t} - \sigma_{dp}\mathbf{Q}' \tag{13}$$

$\mathbf{Q}$ is the solution vector $[u, p]$ and σ_{dp} is a damping function defined as

$$\sigma_{dp}(r) = \frac{1}{4}\left(1 + \tanh\left(a_o \frac{r - 2r_o}{2\delta_\theta}\right)\right) \tag{14}$$

with $r^2 = x^2 + y^2$ and $a_o = 0.575$.
The disturbance $\mathbf{Q}'$ in the Eqs. (13) is computed at every time step t as follows

$$\mathbf{Q}'_{(t)} = \mathbf{Q}_{(t)} - \left(\alpha \bar{\mathbf{Q}}_{(t-1)} + (1-\alpha)\mathbf{Q}_{(t)}\right) \tag{15}$$

where $\bar{\mathbf{Q}}_{(t-1)}$ is the time-average solution computed in the previous time step and $\alpha = 0.90$. Additionally, was applied in the buffer zone the grid stretching to help to dissipate the large-scale disturbances of the jet flowfield.

5. NUMERICAL RESULTS

5.1 Flow dynamic characteristics of the subsonic round jet

The flow dynamic characteristics of a randomly excited round jet were investigated by the analysis of the streamwise mean velocity U normalized by the inlet mean centerline velocity U_j. In the top view of Fig.2, the longitudinal x-z plane at $y = 0$ depicts the streamwise mean velocity development of the jet flow field. As expected, it was observed a similar behavior of the streamwise mean velocity at the x-y plane at $z = 0$, owing to the axisymmetric structure of the round jet. In the bottom views of Fig.2, the streamwise mean velocity was represented in transverse y-z planes positioned at the locations $x/r_o = 6$, 12, 18 and 24. The potential core (depicted in yellow) is defined as a region with almost unchanged velocity ($U/Uj \geq 0.95$). The potential core region is located near the jet nozzle exit and along the central portion of the jet enclosed by the shear layers, with an axial length $x_c = 12.17$. As show Figs.2a-b, the region of potential core is gradually reduced downstream by the continous increase of the shear layer thickness. The merging of shear layers downstream of the potential core region (Figs.2c-b) gives rise to significant jet spreading and rapid mean velocity decaying.

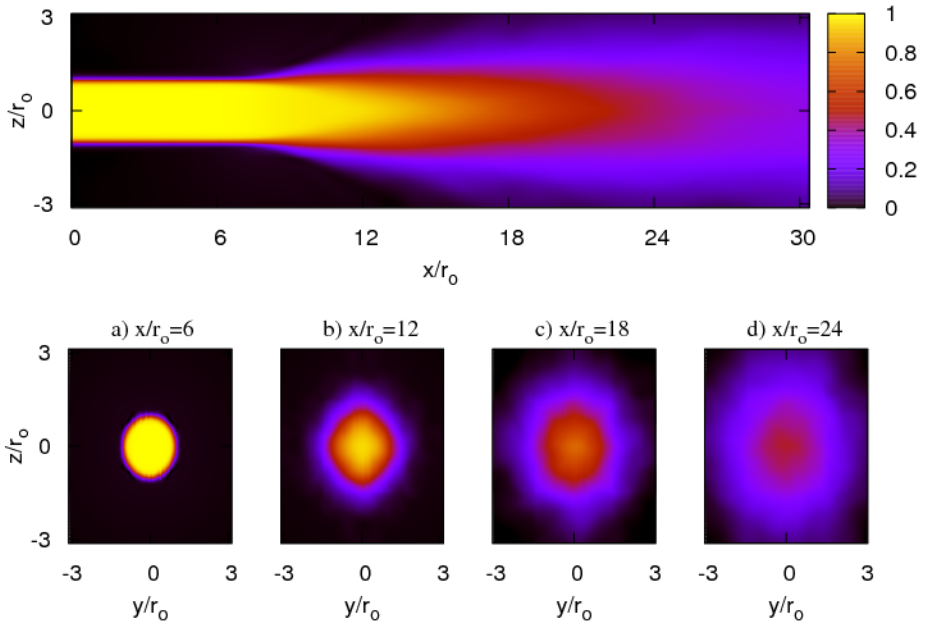

Figure 2. **Mean velocity U normalized by the inlet mean centerline velocity U_j. Top: longitudinal x-z plane at $y = 0$ and bottom: transverse y-z planes at the streamwise locations: $x/r_o = 6$, 12, 18 and 24.**

The mean flow development along the jet centerline computed by implicit LES was compared in Fig.3 with previous results obtained from the literature at similar flow conditions. A small damping in the mean centerline velocity, of around 2.5% of the inlet mean velocity U_j, was observed in the present computations just before the potential core colapse. However, this behavior within the potential core has already been detected experimentally (Islam, M. T. and Ali, M. A. T., 1997) and numerically (Bogey, C. and Bailly, C., 2006). It is important to remark that the mean velocity decayng in the turbulence mixing region obtained by implicit LES presents good agreement with the LES by Bogey, C. (2000) at the same flow conditions (same Mach number and Reynolds number and momentum thickness) and the theoretical decaying law: $U_c/U_j = B/x - x_o$, where $x_o = 0$ is the virtual origin of the jet nozzle and the constant B characterizes the centerline velocity decaying rate. The smaller decaying of curves U_c/U_j obtained by the LES of Uzun *et al.* (2003) and experimentally (Arakeri, V. H. and Krothapalli, A. and Siddavaram, V. and Alkislar, M. B. and Lourencoa, L. M. (2003) and Lau, J. C. and Morris, P. J. and Fisher, M. J. (1993)) is attributed to the smaller viscous dissipation effects associated to the higher Reynolds numbers.

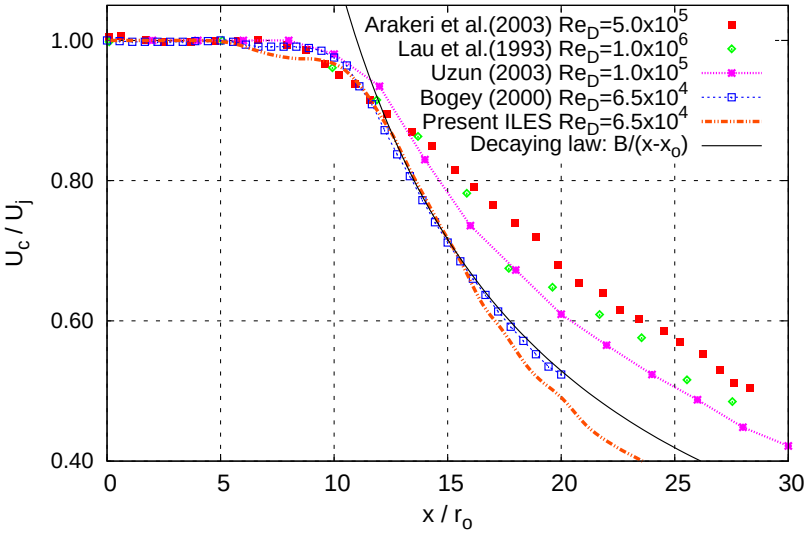

Figure 3. **Mean centerline velocity U_c normalized by the inlet mean centerline velocity U_j. Comparison of the present implicit LES with LES (Bogey, C. (2000) and Uzun *et al.* (2003)), experimental data (Arakeri *et al.* (2003) and Lau *et al.* (1993)) and the theoretical decaying law.**

As shows Table 1, the value of constant $B = 10.9r_o$ computed by implicit LES presents good agreement with results obtained by DNS (Boersma *et al.*, 1998) and LES (Bogey, C., 2000) and experimentally (Wygnanski and Fiedler, 1969; Panchapakesan and Lumley, 1993; Hussein *et al.*, 1994). The jet half-width $\delta_{1/2}$ is a characteristic measurement of the jet spreading defined as the radial location (x, r) where the jet mean velocity $U(x, r) = U(x, r_o)/2$, with $r = (y^2 + z^2)^{1/2}$. In the turbulence mixing region, the jet spreads linearly as $\delta_{1/2}/r_o = A \times (x - x_0)$ where $A \approx 0.074r_o$. It is worth noting that the value of constant A got by the present approach is slightly smaller than the values obtained by experiments, DNS and LES. Nevertheless, this undesirable behavior is being currently investigated and seems to be related to grid dissipation effects associated with the relatively coarser resolution employed in the neighborhood of jet shear layer.

M	Re_D	B/r_o	A/r_o	Methodology	Reference
0.15	8.6×10^4	10.8	0.086	Experiment	Wygnanski & Fiedler (1969)
0.08	1.1×10^4	12.2	0.096	Experiment	Panchapakesan & Lumley (1993)
0.16	9.5×10^4	11.6	0.094	Experiment	Hussein et *al.* (1994)
–	2.4×10^3	11.8	0.095	DNS	Boersma et *al.* (1998)
0.90	6.5×10^4	11.0	0.096	LES	Bogey (2000)
0.90	6.5×10^4	10.9	0.074	Implicit LES	Present approach

Table 1. Mean flow parameters obtained from experiments, DNS, LES and implicit LES.

5.2 Analysis of flow noise-sources and souund propagation

The aerodynamic flow noise-source region and the acoustic field propagation of a randomly excited subsonic round jet were depicted in Fig.4 by the superposition of the instantaneous of vorticity and dilatation fields. The application of a low-amplitude random disturbance near the jet inlet shear layer trigger an earlier startup and growth of Kelvin-Helmolholtz instabilities, which give rise to the evolutive process of rolling up, vortex pairing and merging of two consecutive large-scale vortex structures. The convected large-scale vortex structures are breaking down into smaller-scales vortical structures in the turbulence mixing region, just downstream the potential core. The dissipative nature of the breakdown process continues to generate smaller and smaller scales far downstream. It should be noticed that the dominant noise source in the jet shear layer are the acoustic waves propagating from the region where the vortex-pairing process takes place, without any significant wave oscillations provided by the excitation. The particularly high directivity character of noise radiated, especially noticed at high Mach numbers, is attributed to the axisymmetric quadrupolar nature of jet flow noise-sources (Bogey, C. and Bailly, C., 2003a).

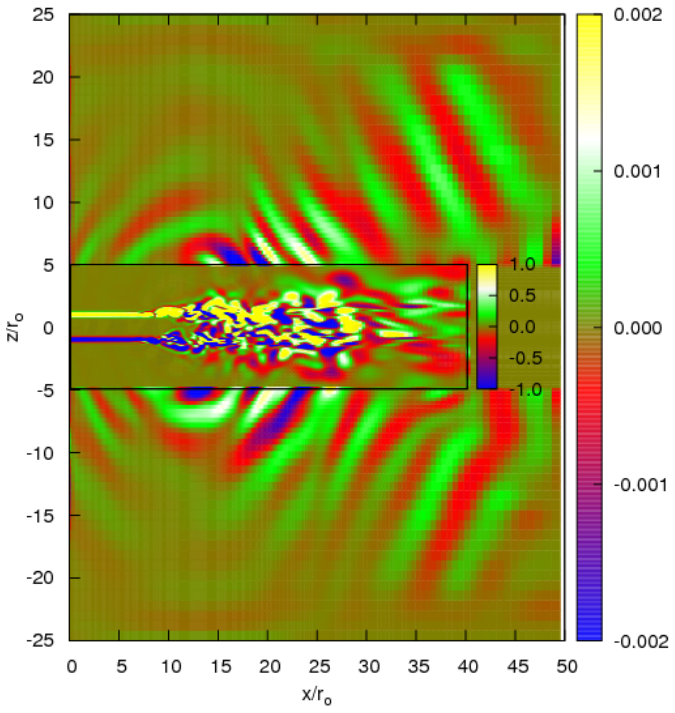

Figure 4. **Visualizations of the aerodynamic flow-noise source region (center) and the acoustic field propagation (outer part of the domain) obtained by superposing snapshots of vorticity and dilatation fields. Representation of the physical domain in the x-z plane at $y = 0$ excluding the region of the buffer zone, located after $x/r_o = 50$.**

6. CONCLUDING REMARKS

An implicit LES/ADM methodology was developed in the present work to perform highly accurate MPI parallel computations of the aerodynamic noise radiated by a randomly excited Mach 0.9 round jet at Reynolds number 6.5×10^4, with inlet shear layer momentum thickness $0.05r_o$. Flow dynamic characteristics, such as the shear-layer momentum thickness, mean centerline velocity decaying and potential core length were found to be in good agreement with previous numerical results and experimental data taken from the literature at similar flow conditions. However, the jet spreading rate is slightly smaller than values obtained by experiments, DNS and LES. The analysis of flow-noise sources and the acoustic field propagation showed that the dominant sound source generated in the jet shear layer is the noise radiated from the region where the vortex pairing process takes place, without any significant spurius wave oscillations provided by the near-inlet random disturbance.

7. ACKNOWLEDGEMENTS

This research project in computational aeroacoustics was supported by the LAE (Laboratory of Aerodynamics) Aeronautical Engineering Department - University of São Paulo, Brazil. The project was sponsored by FAPESP (Fundação de Amparo à Pesquisa do Estado de São Paulo) which we gratefully thank for the financial support.

8. REFERENCES

Arakeri, V. H. and Krothapalli, A. and Siddavaram, V. and Alkislar, M. B. and Lourencoa, L. M., 2003. "On the use of microjets to suppress turbulence in a Mach 0.9 axisymmetric jet". *J. Fluid Mech.*, Vol. 490, No. 75.

Bodony, D. J. and Lele, S. K., 2005. "On using large-eddy simulation for the prediction of noise from cold and heated turbulent jets". *Phys. Fluids*, Vol. 17, pp. 85–103.

Boersma, B.J., Brethouwer, G. and Nieuwstadt, F., 1998. "A numerical investigation on the effect of the inflow conditions on a self-similar region of a round jet". *Phys. Fluids*, Vol. 10, pp. 899–909.

Boersma, B. J. and Lele, S. K., 1999. "Large eddy simulation of Mach 0.9 compressible jet". *AIAA paper 99-1874*.

Bogey, C., 2000. *Calcul direct du bruit aérodynamique et validation de modèles acoustiques hybrides*. Thesis, École Centrale de Lyon, Lyon - France.

Bogey, C. and Bailly, C., 2002. "Direct computation of the sound radiated by a high- Reynolds-number, subsonic round jet". In *CEAS Workshop From CFD to CAA*.

Bogey, C. and Bailly, C., 2003a. "LES of a high Reynolds, high subsonic jet : effects of the inflow conditions on flow and noise". In *AIAA, Paper No. 2003-3170*.

Bogey, C. and Bailly, C., 2003b. "LES of a high Reynolds, high subsonic jet : effects of the subgrid modellings on flow and noise". *AIAA, Paper No. 2003-3557*.

Bogey, C. and Bailly, C., 2005. "Effects of inflow conditions and forcing on subsonic jet flows and noise". *AIAA J.*

Bogey, C. and Bailly, C., 2006. "Computation of a high Reynolds number jet and its radiated noise using large eddy simulation based on explicit filtering". *Computat. Fluids*, Vol. 33, pp. 1344–1358.

Bogey, C. and Bailly, C. and Juvé, D., 2003. "Noise investigation of a high subsonic, moderate Reynolds number jet using a compressible large eddy simulation". *Theor. Comput. Fluid Dyn.*, Vol. 16, No. 4, pp. 273–297.

Brown, C.A., 2005. "Acoustics of excited jets - a historical perspective". *Technical memorandum No. 213889, NASA-Glenn Research Center*.

Choi, D. and Barber, T. J. and Chiappetta, L. M., 1999. "Large eddy simulation of high-Reynolds number jet flows". *AIAA paper 99-0230*.

Colonius, T. and Lele, S. K. and Moin P., 1993. "Boundary condition for direct computation of aerodynamic sound generation".

Colonius, T. and Lele, S. K. and Moin P., 1997. "Sound generation in a mixing layer". *J. Fluid Mech.*, Vol. 330, pp. 375–409.

Gaitonde, D. V. and Visbal, M. R., 1998. "High-order schemes for Navier-Stokes equations Algorithm and implementation into FDL3DI". *Technical Report AFRLVA-WP-TR-1998-3060, Air Force Research Laboratory, Wright-Patterson, AFB*.

Gaitonde, D. V. and Visbal, M. R., 1999. "Further development of a Navier-Stokes solution procedure based on higher-order formulas". *AIAA Paper No. 99-0557*.

Galdi, G. P., 2000. In *Lectures in Mathematical Fluid Dynamics*. Birkhäuser-Verlag, Basel, Switzerland.

Germano, M. and Piomelli, U. and Moin, P., 1991. "A dynamic subgrid-scale eddy viscosity model". *Phys. Fluids A*, Vol. 3, pp. 1760–1765.

Hussein, J., Capp, S. and George, H., 1994. "Velocity measurements in a high-Reynolds-number, momentum-conserving, axisymmetric, turbulent jet". *J. Fluid Mech.*, Vol. 258, pp. 31–75.

Islam, M. T. and Ali, M. A. T., 1997. "Mean velocity and static pressure distributions of a circular jet". *AIAA J*, Vol. 35, pp. 196–197.

Lau, J. C. and Morris, P. J. and Fisher, M. J., 1993. "Measurements in subsonic and suprsonic free jets using a laser velocimeter". *J. Fluid Mech*, Vol. 1, pp. 1–27.

Lele, S. K., 1992. "Compact finite difference schemes with spectral like resolution". *J. Comput. Phys.*, Vol. 103, pp. 16–42.

Leonard, A., 1974. "Energy cascade in large eddy simulations of turbulent fluid flows". *Adv. Geophys*, Vol. 18A, pp. 237–248.

Lighthill, M.J., 1952. "On sound generation aerodynamically. Part I:. General theory". *Proc. Roy. Soc. London*, Vol. A211, pp. 564–587.

Lilly, D., 1992. "A proposed modication of germano subgrid-scale closure method". *Phys. Fluids*, Vol. 4, pp. 633–635.

Mitchell, B. E. and Lele, S. K. and Moin P., 1999. "Direct computation of the sound generated by vortex pairing in an axisymmetric jet". *J. Fluid Mech.*, Vol. 383, pp. 113–114.

Moser, C. and Lamballais, E. and Gervais, Y., 2006. "Direct computation of the sound generated by isothermal and non-isothermal mixing layers". *The 12th AIAA/CEAS Aeroacoustic conference, AIAA 2006-2447*.

Panchapakesan, N. and Lumley, J., 1993. "Turbulence measurements in axisymmetric jets of air and helium. I - Air jet. II - Helium jet". *J. Fluid Mechanics*, Vol. 246, pp. 197–223.

Park, N. and Lee, S. and Choi, H., 2006. "A dynamic subgrid-scale eddy-viscosity model with a global model coefficient". *Phys. Fluids*, Vol. 18, pp. 125–129.

Sagaut, P., 2001. "Large eddy simulation for incompressible flows". *Springer Verlag*.

Stanley, S.A. and Sarkar, S., 2000. "Influence of nozzle conditions and discrete forcing on turbulent planar jets". *AIAA J.*, Vol. 38, No. 1615.

Stolz, S. and Adams, N.A., 1999. "An approximate deconvolution procedure for large eddy simulation". *Phys. Fluids A*, Vol. 11, pp. 1699–1701.

Stolz, S. and Adams, N.A. and Kleiser, L., 2001a. "An approximate deconvolution model for large-eddy simulations of compressible flows and its application to shock-turbulent-boundary-layer interaction". *Phys. Fluids*, Vol. 13, pp. 2985–3001.

Tanna, H. K., 1977. "An experimental study of jet noise. part i: Turbulent mixing noise". *J. Sound Vib.*, Vol. 50, pp. 405–428.

Uzun, A., Blaisdell, G.A. and Lyrintzis, A.S., 2003. "3-D large eddy simulation for jet aeroacoustics". *9th AIAA/CEAS Aeroacoustics conference, No. 3322 in AIAA 2003, Hilton Head, South Carolina*.

Vreman, A. W., 2004a. "An eddy-viscosity subgrid-scale model for turbulent shear flow: algebraic theory and applications". *Phys. Fluids A*, Vol. 16, No. 10, pp. 3670–3681.

Wygnanski, I. and Fiedler, H., 1969. "Some measurements in the self-preserving jet". *J. Fluid Mech.*, Vol. 38, No. 3, pp. 577–612.

Zaman, K.B.M.Q., 1985. "Far-field noise of a subsonic jet under controlled excitation". *J. Fluid Mech.*, Vol. 152, pp. 83–111.

9. Responsibility notice

The authors are the only responsible for the printed material included in this paper